

# AN INVESTIGATION INTO THE MOMENTUM DISTRIBUTION IN LIGHT NUCLEI

C. M. PUJARA AND K. M. GATHA

DEPARTMENT OF PHYSICS, INSTITUTE OF SCIENCE, BOMBAY

(Received, March 3, 1959)

**ABSTRACT.** The characteristic nuclear density distribution for light elements has been obtained by Gatha and Shah. Using this density distribution, the nucleonic momentum distributions have been obtained on the basis of the Thomas-Fermi-Weizsäcker method for carbon and oxygen. Using these momentum distributions the proton energy spectra, resulting from the inelastic scattering at 30° and 40° of 340 Mev protons by these elements, have been calculated. Using the momentum distribution for carbon, the production efficiencies and the meson energy spectra at 45°, 90° and 135°, resulting from the photo-production of mesons on carbon, have also been calculated.

## I. INTRODUCTION

According to the commonly accepted nuclear model, a nucleus is regarded as composed of nucleons. These nucleons are confined within the nuclear volume. The linear dimensions of such a nuclear region are of the order of  $10^{-13}$  cm. For a nucleon confined in such a region there would be a corresponding uncertainty in its momentum according to the uncertainty principle. The corresponding uncertainty in the kinetic energy of a nucleon can be estimated to be of the order of several million electron volts.

If the exact nuclear wave function is known for the ground state of the nucleus, the corresponding nuclear momentum distribution can be determined through the transformation of the same to momentum space. However, such a nuclear wave function cannot be obtained at present for any complex nucleus. Therefore, it is necessary to obtain the nucleon momentum distribution by some appropriate approximation.

An approximate relation between the nuclear density distribution and nuclear momentum distribution is provided by the Thomas-Fermi method, as discussed by Coulson and March (1950). Some improvements of this method have been suggested by Plaskett (1953) as well as by Weizsäcker (1935). An attempt has been made in this investigation to provide an approximate three-dimensional form to the Plaskett method on the basis of certain assumptions. The Thomas-Fermi method, the Thomas-Fermi-Weizsäcker method and the modified Plaskett method have been tested for the determination of the nuclear momentum distribution assuming an isotropic harmonic oscillator potential. It has been found that the Thomas-Fermi-Weizsäcker method provides the best

results. The Thomas-Fermi-Weizsäcker method has been used in the present investigation for determining the nuclear momentum distributions.

Using the characteristic nuclear density distribution for light elements, determined by Gatha and Shah, the corresponding nuclear density distributions for carbon and oxygen have been calculated and used in this investigation to determine their respective nuclear momentum distributions.

The nuclear momentum distribution can be expected to affect significantly those nuclear reactions where the interaction energy is comparable to the kinetic energy of the nucleon within the nucleus. Cladis, Hess and Moyer (1952) have observed the proton energy spectra for the nuclear inelastic scattering of 340 Mev protons at  $30^\circ$  by carbon and at  $40^\circ$  by carbon and oxygen. At the same time, McMillan, Peterson and White (1949), Steinberger and Bishop (1952), Peterson, Gilbert and White (1951) as well as Sargent Janes and Kraushaar (1954) have observed the pion energy spectra at fixed angles for carbon for the photo-production by bremsstrahlung photons. Some estimates of pion production efficiency have also been reported by some of the above workers. Jenkins, Luckey, Palfrey and Wilson (1954) as well as Luckey (1955) have reported some observations on the pion production efficiency during the photo-production by carbon at certain photon energies.

The above experimental data have been so far correlated on the basis of some assumed nuclear momentum distributions. Cladis *et al* (1952) have used the Gaussian as well as the Chew-Goldberger distributions. They find that the latter distribution is inappropriate while the former distribution, with a kinetic energy half-width of 14 to 19 Mev, is quite suitable for this purpose. Wolff (1952) has correlated the same data on the basis of Chew-Goldberger (1950), Fermi, (1936) as well as Gaussian nuclear momentum distributions. He concludes that the Gaussian nuclear momentum distributions, with a kinetic energy half-width of 12 to 20 Mev, appear appropriate for this purpose. Lax and Feshbach (1951), on the other hand, claim to have reasonably correlated some experimental data on the photo-production of positive pions on carbon by using the Chew-Goldberger distribution.

The purpose of the present investigation has been to correlate the above experimental data on the basis of the nuclear momentum distributions determined from the characteristic nuclear density distribution of Gatha and Shah through the Thomas-Fermi-Weizsäcker method. For this purpose, the theoretical methods developed by Wolff (1952) as well as Lax and Feshbach (1951) have been employed for correlating the respective experimental data with these nuclear momentum distributions.

Therefore, it is concluded that the characteristic nuclear density distribution for light elements, determined by Gatha and Shah, provides at least approximate nuclear momentum distributions for such elements.

## II. NUCLEAR MOMENTUM DISTRIBUTIONS

## A. Characteristic nuclear density distribution

A characteristic nuclear density distribution can be defined by  $\rho(r) = \rho(\bar{r})$ , where  $\rho(r)$  is the nuclear density distribution for any particular element, while  $\rho(\bar{r})$  is the nuclear density distribution for all elements, with  $r$  representing the radial distance from the nuclear centre and  $\bar{r} = rA^{-1/3}$ . Gatha and Shah have determined an improved characteristic nuclear density distribution by eliminating the effects of the higher Born approximations on the nuclear scattering of 340 Mev protons. This characteristic nuclear density distribution is given by

$$\rho(\bar{r}) = \alpha_1 \rho^{-\beta_1 \bar{r}^2} + \alpha_2 \rho^{-\beta_2 \bar{r}^2} \{1 - \beta_3 \bar{r}^2 + \beta_4 \bar{r}^4\} \quad \dots \quad (1)$$

where

$\alpha_1 = 0.12 \times 10^{39} \text{cm}^{-3};$	$\alpha_2 = 0.25 \times 10^{39} \text{cm}^{-3};$
$\beta_1 = 8.62 \times 10^{26} \text{cm}^{-2};$	$\beta_2 = 1.09 \times 10^{26} \text{cm}^{-2};$
$\beta_3 = 0.44 \times 10^{26} \text{cm}^{-2};$	$\beta_4 = 0.13 \times 10^{52} \text{cm}^{-4}.$

This  $\rho(\bar{r})$  for light elements, shown in figure 1, has been used in the present investigation.

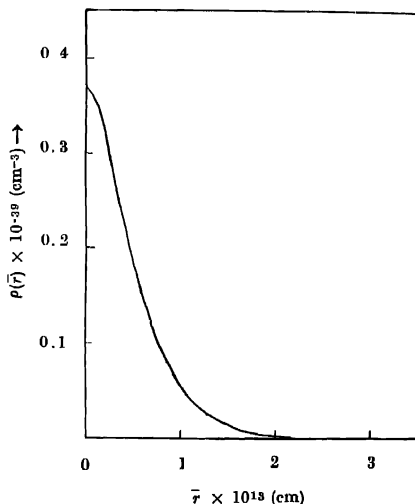


Fig. 1. Characteristic nuclear density distribution for light nuclei.

## B. Thomas-fermi method

A simple relation between the spherically symmetric nuclear density distribution  $\rho(r)$  for proton or neutron, normalised to the number of particles  $N$ , and

the corresponding nuclear maximum momentum distribution  $p_m(r)$  within the nucleus is given by Coulson and March (1950) as

$$\rho(r) = \frac{1}{3\pi^2\hbar^3} p_m^3(r) \quad \dots (2)$$

Defining  $I(p)dp$  as the probability of one nucleon having its absolute momentum between  $p$  and  $p+dp$ , one can write

$$I(p)dp = \int_0^{r(p)} \frac{I_r(p)dp\rho(r)}{N} \cdot 4\pi r^2 dr \quad \dots (3)$$

where  $I_r(p)dp$  is the probability of the nucleon at  $r$  having its absolute magnitude of momentum between  $p$  and  $p+dp$ , and  $r(p)$  has to be determined from the function  $p_m(r)$ . Substituting  $I_r(p)dp$  and  $\rho(r)$  in equation (II, 3), one finds

$$I(p) = \frac{4}{3\pi\hbar^3} \cdot \frac{r^3(p)}{N} \cdot p^2 \quad \dots (4)$$

March (1954) has tested the validity of the Thomas-Fermi method for the nuclear problem by assuming an isotropic harmonic oscillator nuclear potential. He finds that there is a close agreement for medium and heavy nuclei, while the method needs some improvement for light nuclei. He further points out that  $I(p)$ , obtained by this method, is particularly unreliable for very small and very large momenta.

It may be noted that, for a characteristic nuclear density distribution, one can rewrite equation (II, 4) to have

$$I(p) = \frac{4\pi^3(p)p^2}{3\pi\hbar^3} \quad \dots (5)$$

### C. Thomas-Fermi-Weizsäcker method

Weizsäcker's method, for a single type of particle without spin, can be derived from the variation principle

$$\delta \int \left( \frac{\pi^2\hbar^2}{6M} \rho^3 + \rho V + \frac{\hbar^2}{8M} \frac{\rho'^2}{\rho^2} \right) dx = 0 \quad \dots (6)$$

where  $\rho$  is the particle density and  $V$  is the potential energy. It may be noted that the last term alone represents the correction introduced by Weizsäcker. The corresponding Euler equation gives

$$\frac{\pi^2\hbar^2}{2M} \rho^2 + V - \frac{\hbar^2}{4M} \frac{\rho''}{\rho} + \frac{\hbar^2}{8M} \frac{\rho'^2}{\rho^2} = E \quad \dots (7)$$

where  $E$  is the Lagrange multiplier of the dimensions of energy.

Plaskett (1953), using a more fundamental analysis, obtains

$$\frac{\pi^2\hbar^2}{2M} \rho^3 + V + \frac{\hbar^2}{4M} \frac{\rho''}{\rho} - \frac{3\hbar^2}{8M} \frac{\rho'^2}{\rho^2} = E \quad \dots (8)$$

Ballinger and March (1954) have tested both these methods by comparing the particle density given by them for an oscillator potential with the exact density for the same. They indicate that the Weizsäcker method provides the appropriate behaviour for the density for small as well as large distances. It may, therefore, be expected that the Weizsäcker method may provide an appropriate behaviour for  $I(p)$  for small as well as large momenta. Therefore the Thomas-Fermi-Weizsäcker method has been used in the present investigation for determining the nuclear momentum distributions from the nuclear density distributions.

The Thomas-Fermi-Weizsäcker method for the nuclear problem, in three dimensions, can be derived from the variation principle

$$\delta \int \left[ \frac{\pi^2 \hbar^2}{10M} \left( \frac{3}{\pi} \right)^{5/3} (\rho_P^{5/3} + \rho_N^{5/3}) + (\rho_P + \rho_N) V + \frac{\hbar^2}{8M} \left\{ \frac{(\nabla \rho_P)^2}{\rho_P} + \frac{(\nabla \rho_N)^2}{\rho_N} \right\} \right] d\vec{r} = 0 \quad \dots (9)$$

where  $\rho_P$  and  $\rho_N$  are the proton and neutron densities. Following Gombas (1952), it will be assumed that  $\rho_P = \rho_N = \rho/2$ . Thus one has

$$\delta \int \left[ \frac{\pi^2 \hbar^2}{5M} \left( \frac{3}{2\pi} \right)^{5/3} \rho^{5/3} + \rho V + \frac{\hbar^2}{8M} \frac{(\nabla \rho)^2}{\rho} \right] d\vec{r} = 0 \quad \dots (10)$$

Thus the above equation can be written as

$$\delta \int F(\rho, \rho') d\vec{r} = 0 \quad \dots (11)$$

where,

$$F(\rho, \rho') = \frac{\pi^2 \hbar^2}{5M} \left( \frac{3}{2\pi} \right)^{5/3} \rho^{5/3} + \rho V + \frac{\hbar^2}{8M} \frac{(\nabla \rho)^2}{\rho}$$

The Euler equation for such a variation principle can be written as

$$\frac{\partial F}{\partial \rho} - \nabla \cdot \left\{ \frac{\partial F}{\partial (\nabla \rho)} \right\} = E \quad \dots (12)$$

where  $E$  appears as the Lagrange multiplier of the dimensions of energy. In the Thomas-Fermi-Weizsäcker formalism,  $E$  can be regarded as the maximum effective nucleonic energy within the nucleus. This assumption, which has no clear theoretical justification, has been empirically found to improve upon the Thomas-Fermi method in respect of the nuclear momentum distribution. Assuming  $V$  to be independent of any small variation of  $\rho$ , as well as considering  $\rho$  and  $V$  spherically symmetrical, one can write

$$p_m = \left[ (3\pi^2)^{2/3} \hbar^2 \rho^{2/3} + \frac{\hbar^2}{4} \left( \frac{\rho'}{\rho} \right)^2 - \frac{\hbar^2}{2} \frac{\rho''}{\rho} - \frac{\hbar^2}{r} \frac{\rho'}{\rho} \right]^{1/2} \quad \dots (13)$$

The above  $p_m(r)$  may be used, along with equation (II, 3) to determine the shapes of the nuclear momentum distributions. Such nuclear momentum distributions require suitable renormalization, as  $p_m(r)$  is no longer connected with  $\rho(r)$  through the equation (II, 2).

#### D. Plaskett method

The Thomas-Fermi method, in one dimension, has been sought to be replaced by Plaskett (1953). It has not been possible for him to obtain a three dimensional form. In analogy with Plaskett's method in one dimension, an approximate relation in three dimensions has been set up in this investigation.

The Schrödinger equation in three dimensions is given by

$$\left[ -\frac{\hbar^2}{2M} \nabla^2 - g(\bar{r}) \right] \psi(\bar{r}) = 0 \quad \dots (14)$$

where  $g(\bar{r}) = E - V(\bar{r})$ . One may now require that the solution of the above equation has the form

$$\psi(\bar{r}) = A(\bar{r}) \rho^{(i/\hbar)} \int_{\bar{r}}^{\bar{r}} \bar{P}(\bar{\xi}) \cdot d\bar{\xi} \quad \dots (15)$$

Substituting the solution given in equation (11, 15) into equation (II, 14) and separating the real and the imaginary parts, one obtains the simultaneous equations

$$A \bar{\nabla} \cdot \bar{P} + 2\bar{P} \cdot \bar{\nabla} A = 0 \quad \dots (16)$$

$$2Mg = P^2 - \hbar^2 \Delta A / A \quad \dots (17)$$

One may note that

$$\frac{\bar{\nabla} A}{A} = \left( \frac{\bar{\nabla} A}{A} \right)^2 + \bar{\nabla} \cdot \left( \frac{\bar{\nabla} A}{A} \right) \quad \dots (18)$$

which by equation (II, 16) leads to

$$\frac{\bar{\nabla} A}{A} = \frac{1}{4} \left( \frac{\bar{\nabla} \cdot \bar{P}}{\bar{P}} \right)^2 - \frac{1}{2} \bar{\nabla} \cdot \left( \frac{\bar{\nabla} \cdot \bar{P}}{\bar{P}^2} \bar{P} \right) \quad \dots (19)$$

Substituting equation (II, 19) into equation (II, 17) one has

$$2Mg = P^2 - \frac{\hbar^2}{4} \left( \frac{\bar{\nabla} \cdot \bar{P}}{\bar{P}} \right)^2 + \frac{\hbar^2}{2} \bar{\nabla} \cdot \left( \frac{\bar{\nabla} \cdot \bar{P}}{\bar{P}^2} \bar{P} \right) \quad \dots (20)$$

Applying the above equation to the motion of the nucleon with the highest energy, one may require that it should revert to the Thomas-Fermi relation when  $\bar{P}$  is a slowly varying function of  $\bar{r}$ . By using equation (II, 2), one has

$$P^2 = (3\pi^2 \hbar^3)^{2/3} \rho^{2/3} \quad \dots (21)$$

Thus a connection can be established between the magnitude of  $\bar{P}$  and  $\rho$ . However, this does not give any information regarding the directional properties of  $\bar{P}$ . Therefore, it is not possible to make use of equation (II, 20) directly.

One may make a simplifying assumption that  $\bar{P}$  varies slowly in direction. To introduce this assumption one can rewrite (II, 16) as

$$\nabla \cdot (A^2 \bar{P}) = 0 \quad \dots \quad (22)$$

One may also note that

$$\nabla \cdot \left( \frac{\bar{P}}{\bar{P}} \right) = \nabla \cdot \bar{n} = 0 \quad \dots \quad (23)$$

where  $\bar{n}$  is a unit vector in the direction of  $\bar{P}$ , provided the directional variation of  $\bar{n}$  is slow as assumed. Comparing equation (II, 22) with equation (II, 23), one can write  $A = CP^{-1}$  where  $C$  is an undetermined constant.

Substituting the value of  $A$  and  $P^2$  into equation (II, 17) and replacing  $2Mg$  by  $p_m^2$ , one obtains

$$p_m^2 = P^2 - \hbar^2 P^4 \Delta(P^{-1}) \quad \dots \quad (24)$$

Substituting into equation (II, 24) from equation (II, 21) and considering  $\rho$  and  $P$  spherically symmetrical, one obtains

$$p_m = \left[ (3\pi^2 \hbar^3)^{2/3} \rho^{2/3} + \frac{\hbar^2}{3r} \frac{\rho'}{\rho} - \frac{7\hbar^2}{36} \left( \frac{\rho'}{\rho} \right)^2 + \frac{\hbar^2}{6} \frac{\rho''}{\rho} \right]^{1/2} \quad \dots \quad (25)$$

where  $\rho'$  and  $\rho''$  are the first and the second radial derivatives of  $\rho$  respectively.

The above  $p_m(r)$  may be used along with the equation (II, 3) to determine the nuclear momentum distributions. Such nuclear momentum distributions would also require renormalization as mentioned before.

## II. Application to isotropic harmonic oscillator

The nuclear density distribution, used in the present investigation, is similar in form to the particle density distribution in an isotropic harmonic oscillator potential. Therefore it is advisable to test the applicability of the various methods for determining the nuclear momentum distributions by considering such an isotropic harmonic oscillator. Such tests can be carried out because it is possible to calculate the particle density distribution as well as the corresponding particle momentum distribution exactly in this instance,

March (1954) has carried out such tests for the Thomas-Fermi method by considering 20, 58 and 92 protons or neutrons. Since only carbon and oxygen nuclei have been tested in the present investigation, only 6 or 8 protons or neutrons need be considered in this connection. Since the case of 8 protons or neutrons would provide completed shells, only such a case has been treated here for simpli-

city. The Thomas-Fermi method, the Thomas-Fermi-Weizsäcker method and the modified Plaskett method have also been tested.

Morse and Feshbach (1953) have given, for an isotropic harmonic oscillator, the expression for  $\psi_{nlm}(r, \theta, \phi)$ . Similarly Morse and Feshbach (1953) have also given the corresponding expression for  $\chi_{nlm}(p, \theta, \phi)$ . Both these expressions needed some small corrections for proper normalization. Using such corrected expressions and taking  $\rho_{nlm}(r, \theta, \phi) = |\psi_{nlm}(r, \theta, \phi)|^2$  and  $I_{nlm}(p, \theta, \phi) = 4\pi p^2 |\chi_{nlm}(p, \theta, \phi)|^2$ , one has in terms of dimensionless quantities,

$$\xi_{nlm}(t, \theta, \phi) = \frac{\pi^{\frac{1}{2}}}{2} (2l+1) \frac{(l-|m|)!}{(l+|m|)!} \frac{\left(\frac{n}{2} - \frac{l}{2} - \frac{1}{2}\right)!}{\left[\Gamma\left(\frac{n}{2} + \frac{l}{2} + 1\right)\right]^3} t^{2l} e^{-t^2} \times \left[ \frac{L_{\frac{n}{2} - \frac{l}{2} - \frac{1}{2}}^{l+\frac{1}{2}}(t^2)}{\left[\Gamma\left(\frac{n}{2} + \frac{l}{2} + 1\right)\right]^3} \right]^2 \{P_l^m(u)\}^2 \quad \dots \quad (26)$$

$$\eta_{nlm}(s, \theta, \phi) = \frac{\pi^{\frac{1}{2}}}{2} (2l+1) \frac{(l-|m|)!}{(l+|m|)!} \frac{\left(\frac{n}{2} - \frac{l}{2} - \frac{1}{2}\right)!}{\left[\Gamma\left(\frac{n}{2} + \frac{l}{2} + 1\right)\right]^3} s^{2l+2} e^{-s^2} \times \left[ \frac{L_{\frac{n}{2} - \frac{l}{2} - \frac{1}{2}}^{l+\frac{1}{2}}(s^2)}{\left[\Gamma\left(\frac{n}{2} + \frac{l}{2} + 1\right)\right]^3} \right]^2 \{P_l^m(u)\}^2 \quad \dots \quad (27)$$

where  $t = \beta^{\frac{1}{2}} r$ ,  $s = p/\hbar\beta^{\frac{1}{2}}$ , with  $\beta = M\omega/\hbar$  where  $M$  the nucleon mass and  $\omega$  the classical frequency for the oscillator potential. Also  $\xi_{nlm}(t, \theta, \phi) = (\pi/\beta)^{3/2} \rho_{nlm}(r, \theta, \phi)$  and  $\eta_{nlm}(s, \theta, \phi) = (\hbar/4) (\pi/\beta)^{\frac{3}{2}} \times I_{nlm}(p, \theta, \phi)$ , where  $n = \cos \theta$ . Further,  $L$  represents the Laguerre function of the corresponding orders as discussed by Morse and Feshbach. In order to obtain purely radial expressions, it is necessary to average over angular variations. Allowing for two spin orientations, this leads to

$$\bar{\xi}_{nl}(t) = \pi^{\frac{1}{2}} \frac{\left(\frac{n}{2} - \frac{l}{2} - \frac{1}{2}\right)!}{\left[\Gamma\left(\frac{n}{2} + \frac{l}{2} + 1\right)\right]^3} t^{2l} \rho^{-t^2} \left[ \frac{L_{\frac{n}{2} - \frac{l}{2} - \frac{1}{2}}^{l+\frac{1}{2}}(t^2)}{\left[\Gamma\left(\frac{n}{2} + \frac{l}{2} + 1\right)\right]^3} \right]^2 \quad \dots \quad (28)$$

$$\bar{\eta}_{nl}(s) = \pi^{\frac{1}{2}} \frac{\left(\frac{n}{2} - \frac{l}{2} - \frac{1}{2}\right)!}{\left[\Gamma\left(\frac{n}{2} + \frac{l}{2} + 1\right)\right]^3} s^{2l+2} \rho^{-s^2} \left[ \frac{L_{\frac{n}{2} - \frac{l}{2} - \frac{1}{2}}^{l+\frac{1}{2}}(s^2)}{\left[\Gamma\left(\frac{n}{2} + \frac{l}{2} + 1\right)\right]^3} \right]^2 \quad \dots \quad (29)$$



In case of 8 particles only the terms for  $n = 1, l = 0$  and  $n = 2, l = 1$  are necessary. For both cases, one gets  $L_0^1 = \pi^1/2$  and  $L_0^{3/2} = 3\pi^1/4$ . Substituting the above values into equations (II, 28) and (II, 29) and allowing for  $(2l+1)$  degeneracy for values of  $m$ , one has for all the 8 particles.

$$\xi(t) = \rho^{-t^2}(2+4t^2) \quad (30)$$

$$\bar{\eta}(s) = \rho^{-s^2}s^2(2+4s^2) \quad (31)$$

The dimensionless total density  $\xi(t)$  for 8 particles, shown in figure 2, roughly similar in form to the characteristic nuclear density of Gatha and Shah as shown

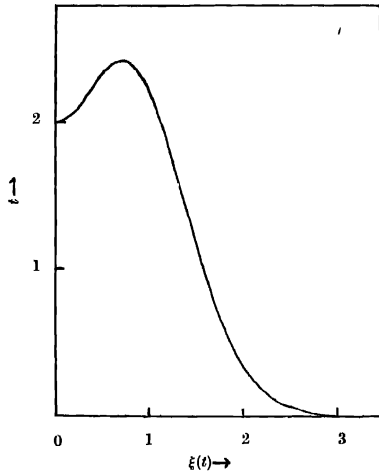


Fig. 2. Dimensionless nuclear density distribution for eight particles in an isotropic harmonic oscillator potential.

in figure 1. This similarity makes the case of the isotropic harmonic oscillator potential useful for testing the applicability of the various methods for the determination of the of the nuclear momentum distributions.

Using Thomas-Fermi method, one has from equation (II, 4) for all the 8 particles

$$\eta_{T.F.}(s) = \frac{s^2}{3\pi^1} \iota^3(s) \quad (32)$$

One has to determine  $\iota(s)$  by using equation (II, 1) in the form

$$s_{T.F.} = [3\pi^1 \xi(t)]^{1/3} \quad (33)$$

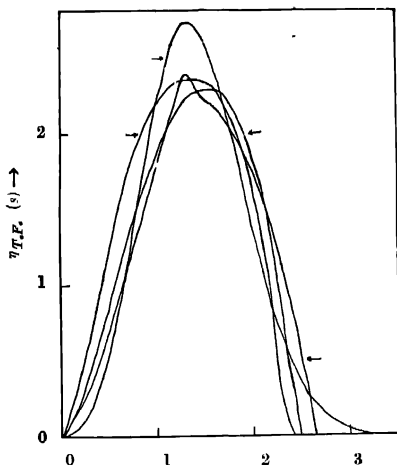


Fig. 3. Dimensionless nuclear momentum distribution for eight particles in an isotropic harmonic oscillator potential.

Top arrow  $\eta$  : By exact method.

Middle left arrow :  $\eta_{T.F.}$  : By Thomas-Fermi method.

Middle right arrow  $\eta_P$  : By Plaskett method

Bottom arrow :  $\eta_{T.F.W.}$  : By Thomas-Fermi-Weizsacker method.

Substituting for  $\xi(t)$  from equation (II, 30) into equation (II, 33)  $t(s)$  has been obtained graphically. Using this  $t(s)$ ,  $\eta_{T.F.}(s)$  has been determined from equation (II, 32). This  $\eta_{T.F.}(s)$  has been shown in figure 3 for comparison with the exact  $\eta(s)$ .

Using Thomas-Fermi-Weizsacker method, one has from equation (II, 3) for all the 8 particles

$$\eta_{T.F.W.}(s) = 3s^2 \int_0^{t(s)} \frac{\xi(t)}{\{s_{T.F.W.}(t)\}^3} t^2 dt \quad \dots \quad (34)$$

where from equation (II, 13), one has

$$s_{T.F.W.} = \left[ \left\{ 3\pi^4 \xi(t) \right\}^{2/3} + \frac{1}{4} \left\{ \frac{\xi'(t)}{\xi(t)} \right\}^2 - \frac{1}{2} \left\{ \frac{\xi''(t)}{\xi(t)} \right\} - \frac{1}{t} \left\{ \frac{\xi'(t)}{\xi(t)} \right\} \right]^{1/2} \quad \dots \quad (35)$$

Similarly using Plaskett method, one has again from equation (II, 3) for all the 8 particles

$$\eta_P(s) = 3s^2 \int_0^{t(s)} \frac{\xi(t)}{\{s_P(t)\}^3} t^2 dt \quad \dots \quad (36)$$

where from equation (II, 25), one has

$$s_P = \left[ \left\{ 3\pi^{\frac{1}{2}} \bar{\xi}(t) \right\}^{\frac{2}{3}} - \frac{7}{36} \left\{ \frac{\bar{\xi}'(t)}{\bar{\xi}(t)} \right\}^2 + \frac{1}{6} \left\{ \frac{\bar{\xi}''(t)}{\bar{\xi}(t)} \right\} + \frac{1}{3t} \left\{ \frac{\bar{\xi}'(t)}{\bar{\xi}(t)} \right\} \right]^{\frac{1}{2}} \quad \dots (37)$$

From these equations  $s_{T.F.W.}(t)$  and  $s_P(t)$  were determined by substituting for  $\bar{\xi}(t)$  from equation (II, 30). The limits  $t'(s)$  for both cases were determined graphically from the corresponding implicit equations (II, 35) and (II, 37). The determination of  $\eta_{T.F.W.}(s)$  and  $\eta_P(s)$  were determined graphically from equation (II, 34) and (II, 36) respectively and the same were renormalized as indicated before. Both  $\eta_{T.F.W.}(s)$  and  $\eta_P(s)$  have been shown in figure 3 along with  $\eta_{T.F.}(s)$  for comparison with the exact  $\bar{\eta}(s)$  determined before.

It is clear from figure 3 that  $\eta_{T.F.}(s)$  is not a very good approximation to  $\bar{\eta}(s)$ . The deviations are particularly apparent both for small and large values of  $s$  as can be expected. It is also clear that  $\eta_P(s)$  deviates even more from  $\bar{\eta}(s)$  at such values of  $s$ . On the other hand,  $\eta_{T.F.W.}(s)$  is closer to  $\bar{\eta}(s)$  for such value of  $s$ . For other values of  $s$ , however it is rather difficult to prefer any one approximation over others. Therefore the behaviour of these approximations for large and small values of  $s$  has been used as a criterion for selection. The Thomas-Fermi-Weizsäcker method is regarded a somewhat superior to others for determining the momentum distribution from the density distribution, of an isotropic harmonic oscillator. Since the nuclear density distribution of Gatha and Shah is of a similar form as the density distribution for the isotropic harmonic oscillator, the Thomas-Fermi-Weizsäcker method has been used, in the present investigation for determining the nuclear momentum distributions.

#### F. Nuclear momentum distributions for carbon and oxygen.

The nuclear momentum distributions for carbon and oxygen have been determined, by using the Thomas-Fermi-Weizsäcker method, from the corresponding nuclear density distributions obtained from the characteristic nuclear density distribution given in equation (II, 1). Since such density distributions pertain to nucleons, one has to modify the expression for the maximum momentum distribution  $p_m(r)$  of equation (II, 13), so as to account for the two isotopic spin states of the nucleons. The expression for  $p_m(r)$  now becomes

$$p_m(\bar{r}) = \left[ \left( \frac{3\pi^2}{2} \right)^{\frac{2}{3}} \bar{\hbar}^2 \rho^{\frac{2}{3}} + \frac{1}{A^{\frac{2}{3}}} \left\{ \frac{\bar{\hbar}^2}{4} \left( \frac{\rho'}{\rho} \right)^2 - \frac{\bar{\hbar}^2}{2} \frac{\rho''}{\rho} - \frac{\bar{\hbar}^2}{r} \frac{\rho'}{\rho} \right\} \right]^{\frac{1}{2}} \quad \dots (38)$$

It may be noted that, in this method,  $p_m(\bar{r})$  is not characteristic although  $\rho(\bar{r})$  is characteristic. Substituting for  $\rho(\bar{r})$  from equation (II, 1),  $p_m(\bar{r})$  was explicitly calculated for carbon as well as oxygen.

In the above notation one can rewrite the expression for nuclear momentum distribution  $I(p)$  from equation (II, 3) as

$$I(p) = 12\pi p^2 \int_0^{\bar{r}(p)} \frac{\rho(\bar{r})}{\{p_m(\bar{r})\}^3} \bar{r}^2 d\bar{r} \quad \dots (39)$$

Using  $\rho(\bar{r})$  of equation (II, 1) and  $p_m(\bar{r})$  as determined before, the momentum distributions  $I_c(p)$  and  $I_o(p)$  for carbon and oxygen respectively were calculated by performing the necessary integrations graphically. It may be noted that these nuclear momentum distributions have to be normalized to unity. Suitable re-normalisations, to this effect, were carried out by multiplying with appropriate normalization constants. Both  $I_c(p)$  and  $I_o(p)$  have been shown in figure 4.

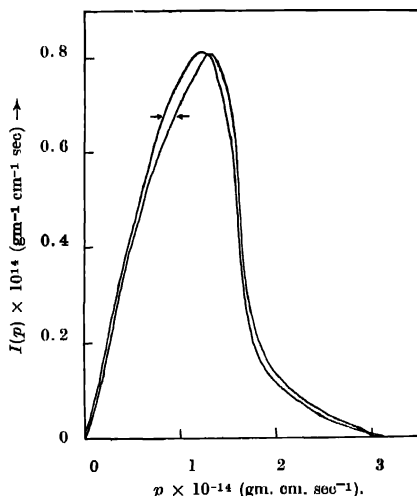


Fig. 4. Nuclear momentum distributions for carbon and oxygen.

→ :  $I_o$  : For oxygen.

← :  $I_c$  : For carbon.

These  $p_m(\bar{r})$  have been used in the present investigation to correlate the experimental data, for carbon and oxygen, on the nuclear inelastic scattering of high energy protons and the photo-production of positive pions.

### III. NUCLEAR INELASTIC SCATTERING OF HIGH ENERGY PROTONS

The proton energy spectra at  $30^\circ$  for carbon and at  $40^\circ$  for carbon and oxygen resulting from the nuclear inelastic scattering of 340 Mev protons from these elements, have been observed by Cladis *et al* (1952). Serber (1947) has proposed a model for the nuclear interactions of high energy nucleons, wherein such

en counters are treated as a series of nucleon-nucleon interactions. For treating such problems, Fermi (1936) first proposed the impulse approximation. Chew (1950) has later elaborated the concepts behind this approximation. On the basis of the above approximation Wolf (1952) has developed an expression for the scattering cross-section  $\sigma(T, \theta)$  for the nuclear scattering of high energy protons. Following Cladis *et al* (1952) this can be simply written as

$$\sigma(T, \theta) = \frac{MA}{2\pi} \int_{-\infty}^{\infty} \frac{I(p)}{P-Q} |\sigma_E(\theta)| \frac{dp}{p} \quad \dots (3.1)$$

where  $M$  = nucleon mass,

$A$  = nuclear mass number,

$I(p) = 4\pi p^2 N(p)$  = nuclear momentum distribution,

$P$  = incident nucleon momentum,

$Q$  = scattered nucleon momentum,

$\sigma_E(\theta)$  = average free nucleon-nucleon scattering cross section at the angle  $\theta$  for the incident energy  $E$ ,

$T$  = scattered nucleon kinetic energy.

The lower limit  $K$  for the above integral has been given by Wolff (1952) as

$$K = [2(P^2 - PQ \cos \theta) - 2\{(P^2 - Q^2)(P^2 + Q^2 - 2PQ \cos \theta)\}^{1/2}]^{1/2} \quad \dots (3.2)$$

The nuclear momentum distributions, determined above, have been used to correlate the experimental data of Cladis *et al* (1952) on the proton energy spectra resulting from the nuclear inelastic scattering of 340 Mev protons by carbon and oxygen. Inserting the values of  $I_c(p)$  and  $I_o(p)$  in equation (II, 39), taking  $\sigma_E(\theta)$  as per Wolff (1952) and calculating  $K$  from equation (II, 38),  $\sigma_c(T, 30^\circ)$ ,  $\sigma_c(T, 40^\circ)$  and  $\sigma_o(T, 40^\circ)$ , for carbon and oxygen as indicated, have been calculated through graphical integration procedures. The observed proton energy spectrum at  $30^\circ$  for carbon is shown in figure 5, while the observed proton energy spectra at  $40^\circ$  for carbon and oxygen are shown in figure 6. The theoretical curve for  $\sigma_c(T, 30^\circ)$  has also been shown in figure 5. Similarly, the theoretical curves for  $\sigma_c(T, 40^\circ)$  and  $\sigma_o(T, 40^\circ)$ , have been shown in figure 6. All the theoretical energy spectra have been shifted along both scales to give the best agreement with the corresponding experimental energy spectra.

It can be seen from figures 5 and 6 that the agreement between the theoretical and the experimental proton energy spectra is about as reasonable as that given by the Gaussian distribution used by Wolff (1952) as well as by Cladis *et al* (1952). However, the peaks in the theoretical spectra, determined in this investigation, are somewhat narrower than those given by the Gaussian distribution. The shapes of such peaks are determined by the nature of the nuclear momentum distributions for very low momenta. At the same time the theoretical spectra, determined in this investigation, deviate slightly more from the experimental spectra than in the case of the Gaussian distribution for very small and very

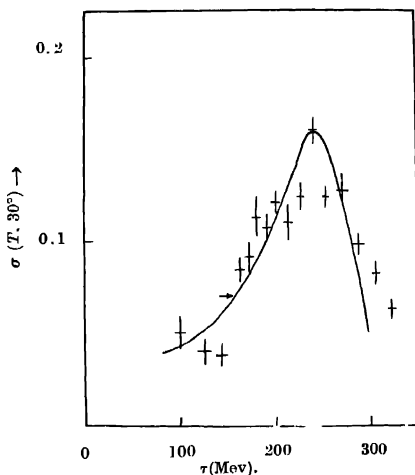


Fig. 5. Relative proton energy spectra at  $30^\circ$  scattering angles from 343 Mev protons on carbon.

$\rightarrow \cdot \sigma_c$  Theoretical energy spectrum.  $+$  Experimental energy spectrum.

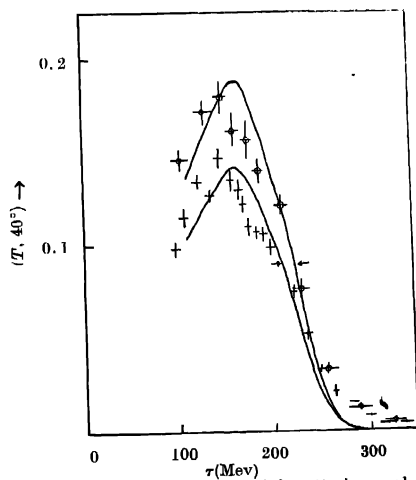


Fig. 6. Relative proton energy spectra at  $40^\circ$  scattering angle from 340 Mev protons on carbon and oxygen.

$\rightarrow$  :  $\sigma_c$  : Theoretical energy spectrum for carbon.  
 $\leftarrow$  :  $\sigma_o$  : Theoretical energy spectrum for oxygen.  
 $+$  : Experimental energy spectrum for carbon.  
 $x$  : Experimental energy spectrum for oxygen.

large  $T$ . The shapes of the theoretical spectra, for such extremal regions, are determined by the nature of the nuclear momentum distributions for very large momenta. It may be noted that all approximate statistical methods, including the Thomas-Fermi-Weizsacker method, for determining the nuclear distribution from the nuclear density distribution are somewhat unreliable for very low and very high momenta. These deviations can, therefore, be presumably ascribed to the failure of the statistical methods for determining the nuclear momentum distributions. Hence, it is reasonable to conclude that the characteristic nuclear density distributions, determined by Gatha and Shah, provides reasonable nuclear momentum distributions from the point of view of the proton energy spectra resulting from the nuclear inelastic scattering of 340 Mev protons by light elements.

#### IV. NUCLEAR PHOTO-PRODUCTION OF HIGH ENERGY PIONS

McMillan *et al* (1949), Steinberger and Bishop (1952), Peterson *et al* (1951) as well as Sargent Janes and Kraushaar (1954) have observed the pion energy spectra at certain definite angles for carbon for the photo-production by bremsstrahlung photons. Attention has been concentrated, in this investigation on the pion energy spectra and pion production efficiency for the photo-production of high energy positive pions by carbon. Some estimates of pion production efficiency have also been reported by some of the above workers. Jenkins *et al* (1954) as well as Luckey (1955) have reported some observations on the pion production efficiency during the photo-production by carbon at certain photon energies. Those observed nuclear reactions can be expected to depend on the nuclear momentum distributions of the elements concerned. Comparing the corrected charged pion energy spectrum at  $90^\circ$  for carbon due to Peterson *et al.* with the positive pion energy spectrum at  $90^\circ$  for carbon due to Sargent Janes and Kraushaar, one finds that the two spectra are considerably inconsistent. In this circumstance, it is natural to place more reliance on the results of electrical measurements than on the results of photographic measurements. Therefore, the pion energy spectra, due to McMillan *et al* and Peterson *et al*, have been disregarded in this investigation. Consequently, the positive pion energy spectrum at  $90^\circ$  for carbon, due to Sargent Janes and Kraushaar has been considered for theoretical interpretation in this investigation. This energy spectrum, as pointed out by Sargent Janes and Kraushaar, give practically no pions below about 8 Mev pion kinetic energy. It is suspected that this may be due to some systematic error of this magnitude in their energy determination. Therefore, this energy spectrum has been shifted towards lower pion kinetic energies by about 8 Mev before comparing the same with the corresponding theoretical energy spectrum in figure 7. Observations have been made for 200 Mev, 235 Mev and 265 Mev

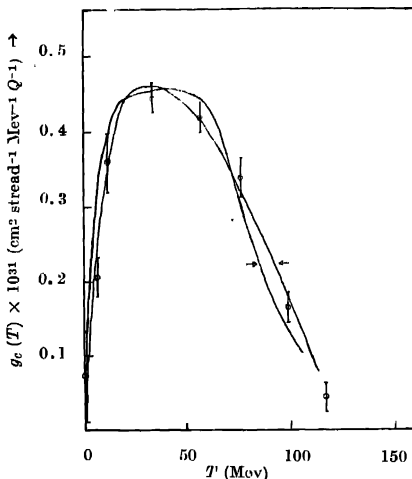


Fig. 7. Positive pion energy spectra at  $90^\circ$  for the photo-production on carbon by 326 Mev Bremsstrahlung photons.

→ :  $G_c$  (Lux) : Theoretical energy spectrum of Lax and Feshbach.

← :  $G_c$  : Present theoretical energy spectrum.

Φ : Experimental energy spectrum.

photons by Jenkins *et al* as well as Luckey for the production efficiencies for the photo-production of positive pions by carbon. From these observations, the differential photo-production cross section  $\sigma_H(\theta)$  for hydrogen, the integrated photo-production cross section  $\sigma_H$  for the same and the angular photo-production efficiency  $\epsilon(\theta)$  for carbon are considered relevant. The differential photo-production cross section  $\sigma_c(\theta)$  per proton for carbon was calculated at various angles by multiplying  $\sigma_H(\theta)$  with the corresponding  $\epsilon(\theta)$ . The probable errors on  $\sigma_c(\theta)$  have been estimated by taking the same fractional errors as shown on their direct measurements of  $\sigma_c(T', \theta)$ . The probable errors on  $\theta$  have also been given by them. Then  $\sigma_c(\theta)$ , obtained above, were graphically integrated after drawing smooth curves through their plots against  $\cos(\theta)$  in the centre of mass system. Finally, the production efficiencies  $\epsilon$  for positive pions for carbon were calculated at these energies by dividing  $\sigma_c$  by the corresponding values of  $\sigma_H$ . These values of  $\epsilon$  at 200 Mev, 235 Mev, and 265 Mev, together with their probable errors, are shown in figure 8 for comparison with the theoretical expression for  $\epsilon$  at such energies.

The theoretical analysis for the nuclear photo-production of positive pions by Hayakawa (1951) as well as Lax and Feshbach (1951) has been based only on formal expressions for the nuclear photo-production of pions by hydrogen, independent of any specific form for the same. Consequently, the theoretical



analysis by Hayakawa has been based on certain assumptions regarding the initial and final nuclear states. He has used the Fermi nuclear momentum distribution only. Lax and Feshbach have carried out their analysis by using the

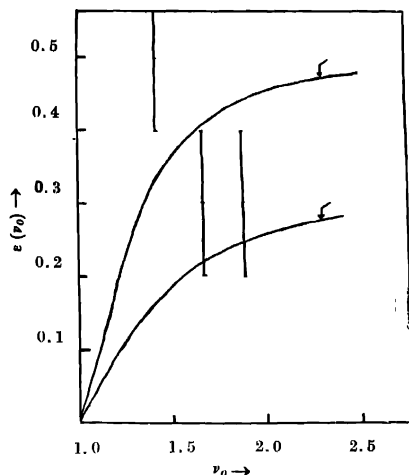


Fig. 8. Positive pion photo-production efficiencies for carbon.

Upper arrow :  $\varepsilon$  : Present theoretical efficiency.

Lower arrow :  $\varepsilon$  : (Lax) : Theoretical efficiency of Lax and Feshbach.

$\phi$  : Experimental efficiency,

closure approximation. The theoretical considerations of Hayakawa as well as Lax and Feshbach lead to similar results, except for the differences pointed out by Marshak (1952). However, the theoretical analysis due to Lax and Feshbach can be applied to any nuclear momentum distribution as illustrated by them. Consequently, the theoretical analysis of Lax and Feshbach has been used in the present investigation.

Lax and Feshbach (1951) have expressed the relative differential cross section as a function of photon and pion energies, for the nuclear photo-production of positive pions, in the dimensionless form

$$g(\nu_0, \mu_0) = (\mu_0^2 - 1)^{1/2} I(\nu_0, \mu_0) / \nu_0 \quad \dots (4.1)$$

where the expression  $I(\nu_0, \mu_0)$  is given by

$$I(\nu_0, \mu_0) = 2\pi \frac{M + \nu_0}{a} \frac{\nu_0}{a} \int_{(b-a) \text{ or } (a^2 - b^2)^{1/2}}^{a+b} \rho(k) k \, dk \quad \dots$$

In these expressions they have taken  $\hbar = C = 1$  and also the pion rest mass

$\mu = 1$ . In these units  $M$  represents the nucleon rest energy, while  $\nu_0$  and  $\mu_0$  represent the photon and the pion energies respectively. At the same time,  $\bar{\nu}$  and  $\bar{\mu}$  represent the photon and the pion momenta respectively. Further,  $\rho(k)$  represents the nuclear momentum distribution. When the incident radiation is a bremsstrahlung spectrum  $f(\nu_0)$  one can obtain the relative differential cross section, as a function of pion energy, by integrating over such a spectrum. Thus one has

$$g(\mu_0) = \int^{\nu_{max}} g(\nu_0, \mu_0) f(\nu_0) d\nu_0 \quad \dots (4.3)$$

where  $\nu_{max}$  is the maximum photon energy for the bremsstrahlung spectrum. According to Marshak (1952), one can use the simple expression,  $f(\nu_0) = 1/\nu_0$ . Since only the relative values of  $g(\mu_0)$  are calculated from equation (IV, 3), normalization of  $f(\nu_0)$  becomes unnecessary.

Using such a bremsstrahlung spectrum with  $\nu_{max} = 2.35$ , Lax and Feshbach (1951) have calculated  $g(\mu_0)$  at  $90^\circ$  for carbon on the basis of the Chew-Goldberger nuclear momentum distribution. Since this theoretical  $g(\mu_0)$  is only relative, it was suitably normalized and compared with the corresponding experimental positive pion energy spectrum of Steinberger and Bishop (1952). A reasonable agreement was obtained between the theoretical and the experimental pion energy spectra. This theoretical pion kinetic energy  $T = \mu c^2(\mu_0 - 1)$  expressed in Mev, has been shown in figure 7. Lax and Feshbach have expressed the positive pion production efficiency, as a function of photon energy, in the form

$$c(\nu_0) = \int \rho(\bar{k}) d\bar{k} \quad \dots (4.4)$$

$$|\bar{\nu} - \bar{k}| \leq [2M(\nu_0 - 1)]^{\frac{1}{2}}$$

where  $\bar{k}$  represents the nucleonic momentum within the nucleus in this units. The production efficiency can be expressed by

$$\epsilon = \frac{\int^{\nu_{max}} \sigma(\nu_0) \epsilon(\nu_0) f(\nu_0) d\nu_0}{\int^{\nu_{max}} \sigma_H(\nu_0) f(\nu_0) d\nu_0} \quad \dots (4.5)$$

where  $\sigma_H(\nu_0)$  is the cross section, per unit photon energy interval at  $\nu_0$ , for the photo-production of positive pions by hydrogen. The monochromatic positive pion production efficiency  $\epsilon(\nu_0)$ , due to Lax and Feshbach, has been shown in figure 8, after reducing the same to half as required by Steinberger and Bishop.

The theoretical positive pion energy spectrum at  $90^\circ$  and the positive pion production efficiency, for the photo-production by carbon, have been obtained in this investigation on the basis of  $I_c(p)$ , determined before, from the theoretical expressions for the same given by Lax and Feshbach.  $N_c(p)$  has been obtained for carbon from  $I_c(p)$  by using the relation  $N_c(p) = I_c(p)/4\pi p^2$ . Using a transformation  $p = \mu ck$ , where  $\mu$  is the pion rest mass,  $\rho_c(k)$  has been obtained from the relation  $\rho_c(k) = (\mu c)^3 N_c(p)$ .

Substituting  $\rho_c(k)$  into equation (IV, 2) and introducing the result into equation (IV, 11 and performing the necessary integration graphically,  $g_c(\nu_0, \mu_0)$  have been determined, for various values of  $\mu_0$ , for each of a set of values of  $\nu_0$ . Next with the bremsstrahlung spectrum defined by  $f(\nu_0) = 1/\nu_0$  and  $\nu_{max} = 2.32$ ,  $g_c(\mu_0)$  has been calculated as a function of  $\nu_0$ . Next,  $g_c(T)$  was obtained by taking pion kinetic energy  $T = \mu c^2(\mu_0 - 1)$  and converting  $T$  to Mev. Since this  $g_c(T)$  is only relative, it has been suitably renormalized and shown in figure 7. It can be seen from figure 7 that the theoretical positive pion energy spectrum, based on the present nuclear momentum distribution, reasonably agrees with the corresponding experimental positive pion energy spectrum. Further,  $g_c(T)$  have also been determined for carbon, at  $45^\circ$  and  $135^\circ$ . These have been shown in figure 9 on an arbitrary scale.

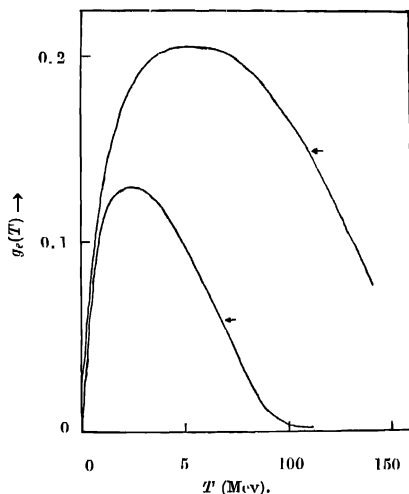


Fig. 9. Theoretical positive pion energy spectra at  $45^\circ$  and  $135^\circ$  for the photo-production on carbon by 326 Mev Bremsstrahlung photons.  
Upper arrow :  $g_c(45^\circ)$ . Lower arrow :  $g_c(135^\circ)$ .

Substituting  $\rho_c(k)$  into equation (IV,4) and performing the necessary integration graphically, the positive pion production efficiency  $\epsilon_p(\nu_0)$  for carbon has been calculated as a function of  $\nu_0$ . This  $\epsilon_p(\nu_0)$ , after reducing the same to half as per the prescription of Steinberger and Bishop, has been shown in figure 8 with the experimental values derived before. It can be seen from figure 8 that the theoretical pion production efficiency for carbon, based upon the present nuclear momentum distribution, roughly agrees with the experimental pion production efficiency.

## CONCLUSION

The nuclear momentum distributions for light elements can be obtained from the characteristic nuclear density distribution on the basis of an empirically reasonable method. Such nuclear momentum distributions can be used for reasonable correlations of the available experimental data on the inelastic nuclear scattering of high energy protons as well as the nuclear photo-production of positive pions by such light elements. Since the theoretical analysis, in each case, has been based on several plausible assumptions and the experimental data contain large errors, it is not possible to discriminate unambiguously between the present momentum distributions and the other proposed nuclear momentum distributions. However, it can be safely concluded that the theoretical deductions, provide at least as good agreement with experimental results as given by any of the proposed nuclear momentum distributions. These conclusions, therefore, further justify the validity of the characteristic nuclear density distribution for light elements employed in the present investigation.

## REFERENCES

- Ballinger, R. A., and March, N. H., 1954, *Proc. Phys. Soc. (London)*, **67**, 378.  
 Chew, G. F. and Goldberger, M. L., 1950, *Phys. Rev.*, **77**, 470.  
 Chew, G. F., 1950, *Phys. Rev.*, **80**, 196.  
 Cladis, J. B., Hess, W. N. and Moyer, B. J., 1952, *Phys. Rev.*, **87**, 425.  
 Coulson, C. A. and March, N. H., 1950, *Proc. Phys. Soc. (London)*, **A63**, 367.  
 Fermi, E., 1936, *Ricerche Sci.* VII-11, 13.  
 Gatha, K. M. and Shah, G. Z., (Private Communication)  
 Gombas, P., 1952, *Acta Phys. Hung.*, **1** 320.  
 Hayakawa, S., 1951, *Phys. Rev.*, **82**, 836.  
 Jenkins, J. L., Luckey, D., Palfrey, T. R. and Wilson, R. R., 1954, *Phys. Rev.*, **95**, 179.  
 Lax, M. and Feshbach, H., 1951, *Phys. Rev.*, **81**, 189.  
 Luckey, D., 1955, *Phys. Rev.*, **97**, 469.  
 Marshak, R. E., 1952, *Meson Physics* (McGraw-Hill, New York.)  
 March, N. H., 1954, *Proc. Phys. Soc. (London)*, **67**, 288.  
 McMillan, E. N., Poterson, V. Z., and White, R. S., 1949, *Science*, **110**, 579.  
 Morse, P. M., and Feshbach, H., 1953, *Methods of Theoretical Physics*, (McGraw-Hill), New York, P. 1663.  
 Morse, P. M. and Feshbach, H., *op. cit.* P. 1679.  
 Morse, P. M. and Feshbach, H., *op. cit.* P. 785.  
 Peterson, J. M., Gilbert, W. S., and White, R. S., 1951, *Phys. Rev.*, **81**, 1003.  
 Plaskett, J. S., 1953, *Proc. Phys. Soc. (London)*, **A66**, 178.  
 Sargent Janes, G., and Kruushaar, W. L., 1954, *Phys. Rev.*, **93**, 900.  
 Serber, R., 1947, *Phys. Rev.*, **72**, 1114.  
 Steinberger, J., and Bishop, A. S., 1952, *Phys. Rev.*, **86**, 171.  
 Weizsäcker Van C. F. V., 1935, *Z. Phys.*, **96**, 431.  
 Wolff, P. A., 1952, *Phys. Rev.*, **87**, 434.